J Sol-Gel Sci Technol (2015) 76:572–581
DOI 10.1007/s10971-015-3807-0

ORIGINAL PAPER

Surfactant-assisted morphological tuning of porous metallic silver sponges: facile synthesis, characterization and catalytic performance

Mehraj Ud Din Sheikh[1] · Gowhar Ahmad Naikoo[1] · Molly Thomas[1] · Mustri Bano[1] · Farid Khan[1]

Received: 19 May 2015 / Accepted: 6 July 2015 / Published online: 26 July 2015

Abstract Nanoporous sponges have many advantages over bulk catalyst structures in terms of providing regular framework of pores and conformational stability. In this paper, precise tuning of porosity and surface morphology in silver sponges for the catalytic reduction of p-nitro phenol to p-amino phenol was explored. The silver spongy catalysts are reusable and stable. The porous catalysts were characterized before calcination by FTIR and TGA and after calcination by XRD, SEM and BET techniques. Catalytic performance of the silver sponges was confirmed by spectrophotometric technique, and it was concluded that the porosity and adsorption capability of silver sponges were responsible for their outstanding catalytic performance.

Graphical Abstract The calcined silver monoliths displayed a potential catalytic activity against the reduction of 4-nitrophenol which is a serious environmental pollutant to 4-aminophenol which is an important intermediate in the synthesis of various analgesic and antipyretic drugs. **Fig. (a)–(e)** Time-dependent successive UV–vis spectra showing the reduction of 4-nitrophenol catalyzed by 0.06 mg of different silver monolith catalysts **(a)** Ag/Triton X-100, **(b)** Ag/Triton X-100/dextran, **(c)** Ag/Triton X-100/TMB, **(d)** Ag/Triton X-100/Ludox (HF treated). **(e)** Plots of A/A_0 versus time of different Ag monoliths for catalytic reduction of 4-nitrophenol (A) Ag/Triton X-100 (B) (C) Ag/Triton X-100/dextran Ag/Triton X-100/TM (D) Ag/Triton X-100/Ludox (HF treated).

✉ Farid Khan
mkzgan@yahoo.com; faridkhan58@yahoo.com; mehrajdavood@gmail.com

[1] Nanomaterials Discovery Laboratory, Department of Chemistry, Dr. Hari Singh Gour Central University, Sagar, M.P. 470003, India

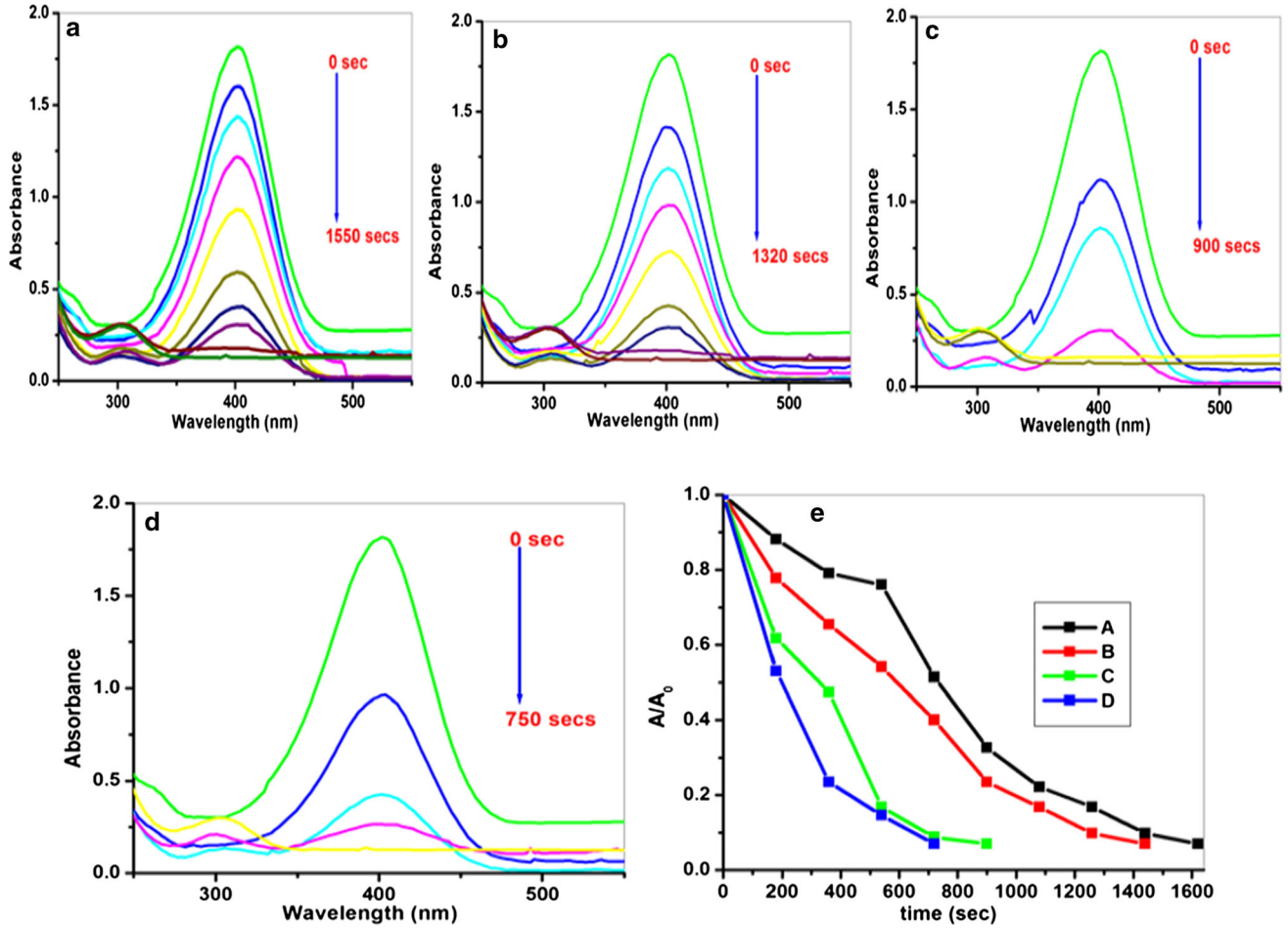

Keywords Porous materials · Triton X-100 · Ag monoliths · Catalysis · Reusability

1 Introduction

In recent years, silver-based materials have been gaining significant research interest due to their unique shape and size-dependent optical [1], antimicrobial [2] and catalytic properties [3]. Nanostructures of silver such as monodispersed nanoparticles [4], nanoprisms [5], nanocubes [6], nanowires [7] and nanodisks [8] have potential applications in optics, catalysis and SERS detection [9].

Hierarchically porous materials with multi-scale porous structure, generally of micro–meso–macroporous nature, have attracted great attention recently due to their dynamic properties such as low density, considerable thermal conductivity [10], gas permeability, bio-filtration capability [11, 12] and adsorption [13, 14]. Hence, such materials are extensively used in heterogeneous catalysis [15–22], biosensor technology [23, 24], electrochemical supercapacitors [25–29], tissue engineering [30], photonic crystals, fuel cell electrodes [21] and chemical separation [11, 12, 31].

Stucky et al. [32] reported the low-temperature liquid crystal like arrays formed by organic molecules and inorganic species like tetraethylorthosilicate. Recently, macroporous monoliths of silver, gold and copper oxide with Triton X-45 have been reported by Khan and Mann [33]. Here we have gone through facile, cost-effective and benign sol–gel method to fabricate different silver monoliths using non-ionic surfactant Triton X-100 as a porogen with different additives to affect the shape and size of pores and hence to modify the surface area which is a prerequisite criterion for heterogeneous catalysis like reduction of 4-nitro phenols. Nitrophenols are severe environmental pollutants due to its anthropogenic, toxic and inhibitory nature so their reduction is very important. But they are used extensively in chemical industries for the manufacture of pesticides, pharmaceutical and synthetic dyes [34–40].

P-aminophenol (PAP) is an important intermediate in the synthesis of various analgesic and antipyretic drugs such as paracetamol, acetanilide and phenacetin. It is also a

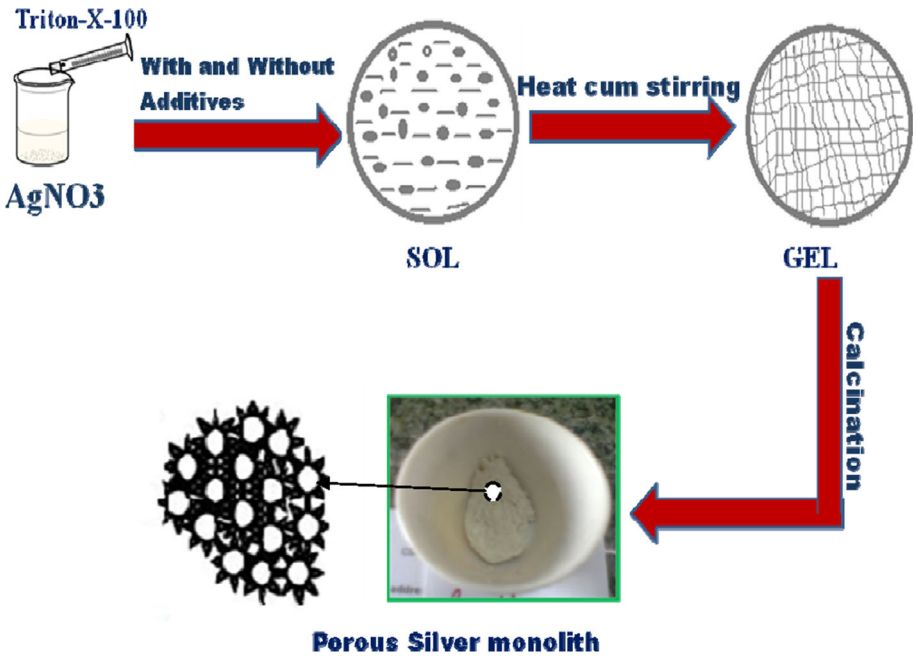

Scheme 1 Synthesis of series of porous silver sponges by using modified sol–gel route

main ingredient in the synthesis of industrial dyes, marketed as a photographic developer, and its oxalate salt is used as a corrosion inhibitor [41]. Based on requirements such as greener route and safer operation, environmentally benign direct catalytic conversion routes have been developed for the conversion of p-nitrophenol to p-aminophenol in aqueous medium under mild conditions. One such route by which p-aminophenol is obtained involves direct hydrogenation of p-nitrophenol using sodium borohydride which is a milder agent, and the reaction can be carried out in aqueous medium [42]. But the sluggish self-hydrolysis of $NaBH_4$ [43] affects the rate of hydrogenation of the nitro compound:

$$NaBH_4(s) + 2H_2O(l) \rightarrow 4H_2O(l) + NaBO_2(aq).$$

Studies reported that the presence of suitable catalysts accelerated the hydrolysis [44]. In this report, catalytic activity of different silver monoliths for the reduction of p-nitrophenol to p-aminophenol process is documented.

2 Experimental

2.1 Materials

Silver nitrate (Sigma-Aldrich as a precursor), soft templates (Triton X-100 Sigma-Aldrich), additives like dextran (Sigma-Aldrich 2×10^{-6} M), 1,3,5-trimethylbenzene (TMB, Merck), Ludox [silica nanoparticles (As-40, colloidal silica, 40 wt% suspension in water, Sigma-Aldrich)] were used as received.

2.2 Synthesis of silver monoliths

In a typical synthesis process, 3.2 g $AgNO_3$ (51.61 wt%, 6.27 M) was dissolved in 3.0 g of water (48.38 wt%) in a 100-ml beaker and added 3.2 g Triton X-100. The resulting gel was stirred for 15 min to form a paste which gradually converted dark in color. The gel was aged for 72 h at room temperature and then calcined at 650 °C for 2 h at a heating rate of 2 °C/min followed by cooling at a rate of 2 °C/min to room temperature in an ELITE furnace. In case of Ag/Triton X-100/dextran, Ag/Triton X-100/TMB and Ag/Triton X-100/Ludox, monoliths were prepared by adding 3.2 g dextran ($Mw = 2 \times 10^6$, 44.44 wt%, 4×10^{-4} M) in 4 g water, 3.46 g TMB (86.5 wt%, 28.78 M), 0.21 g Ludox (4.03×10^2 M, 40 wt% suspension in water) to above protocol separately to Ag/Triton X-100 gel. The whole synthetic procedure is given in Scheme 1.

2.3 Characterizations

FTIR studies were performed on Shimadzu-8400S spectrometer. X-ray diffraction patters were obtained for information regarding the crystallinity of the resultant powders. The measurements were carried out on Bruckner D8 advance diffractometer in the diffraction angle range from $2\theta = 10°$–$90°$, using Cu·Kα radiation at 40 kV and 40 mA. TGA curves were obtained on Perkin-Elmer thermal analyzer using alumina reference crucible at the heating rate of 10 °C/min. The macropores in the monoliths were analyzed using scanning electron microscopy

(SEM). Images were taken on a JEOL 5600 microscope. Nitrogen adsorption–desorption measurements for the surface area determination were performed by an Autosorb-1 instrument (Quantachrome instruments, Inc.) at 77 K.

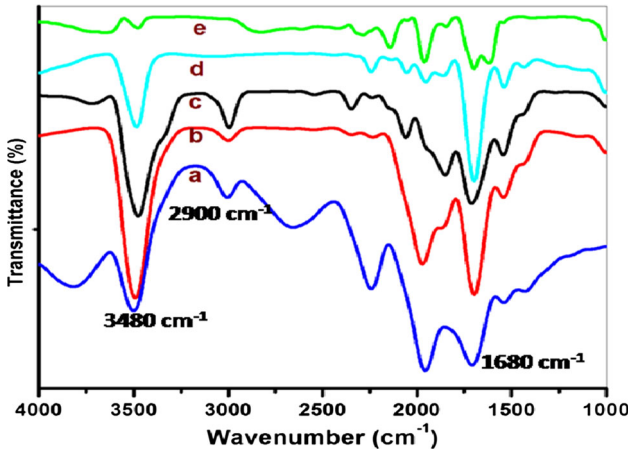

Fig. 1 Fourier transform infrared spectroscopic (FT–IR) studies of Ag xerogels synthesized by Triton X-100 with and without additives *a* Triton X-100, *b* Ag/Triton X-100, *c* Ag/Triton X-100/dextran, *d* Ag/Triton X-100/TMB and *e* Ag/Triton X-100/Ludox

2.4 Catalytic test

The catalytic activity of the synthesized Ag monoliths was studied by carrying out the reduction of 4-NP in the presence of $NaBH_4$. In a typical catalytic reaction, 50 µl of aqueous 4-NP (0.005 M), 0.0038 g $NaBH_4$ (0.0001, 0.010 mol%) powder and 3.05 ml ultrapure water were added in a quartz cuvette, followed by the addition of 0.06 mg of catalyst, and the mixture was quickly subjected to UV–vis measurements (Systronics UV–vis spectrophotometer, 2201). The color change of the solution from yellow to colorless could be clearly observed as the reaction proceeds [45]. The catalytic conversion of 4-NP to 4-aminophenol (4-AP) in presence of excess amount of $NaBH_4$ is shown as:

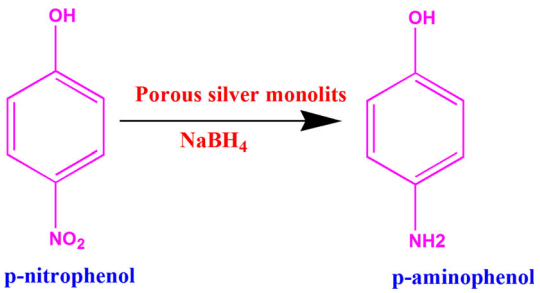

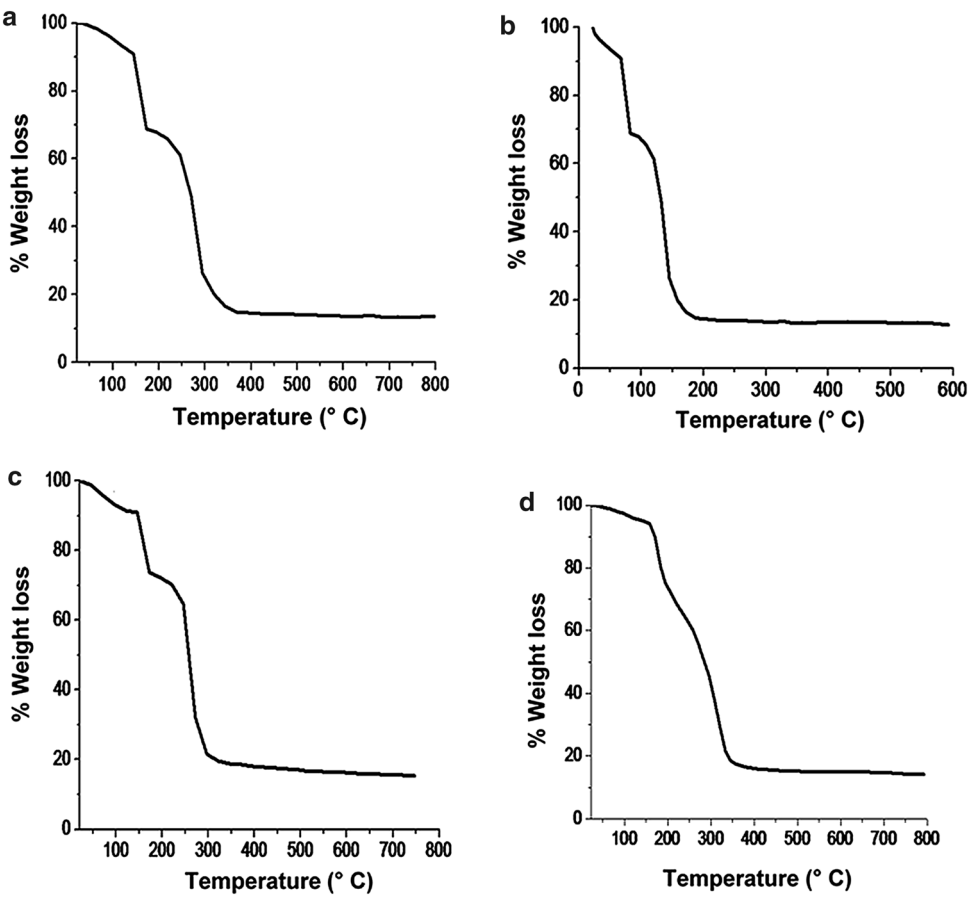

Fig. 2 TGA profiles of Ag gels with and without additives; **a** Ag/Triton X-100, **b** Ag/Triton X-100/dextran, **c** Ag/Triton X-100/TMB and **d** Ag/Triton X-100/Ludox

3 Results and discussion

3.1 FT–IR study

The FTIR frequencies 3480, 2900 and 1680 cm^{-1} corresponding to OH (stretching), CH (stretching) and CO (stretching) of pure surfactant Triton X-100 are shown in Fig. 1a. As the silver ion is reduced to silver monolith by reducing agent Triton X-100, the corresponding frequencies in Ag/Triton X-100 with and without additives are shifted to lower side which is clear from Fig. 1b–d and, hence, confirms the complexation of Ag+ with the used surfactant and additives.

3.1.1 Thermogravimetric analysis (TGA analysis)

TGA curve Ag/Triton X-100 monoliths (Fig. 2a) revealed initial weight drop of 14 % from room temperature to 165 °C due to removal of moisture. A weight drop of 32 % between 190 and 340 °C was shown due to decomposition of $AgNO_3$ and Triton X-100. Finally, 20 % mass of porous silver was left. In case of Ag/Triton X-100/dextran gels (Fig. 2b), initial weight drop of 22 % corresponds to removal of unbounded Triton X-100 from temperature range of 150–180 °C and left 12 % of silver at the end. In case of Ag/Triton X-100/TMB monoliths (Fig. 2c), initial 7 % weight drop was observed up to temperature of 22–160 °C due to loss of moisture followed by weight drop of 18 % at 160–190 °C due to removal of unbounded Triton X-100 and TMB and started leaving 12 % of the silver at the end. Similar TGA curves were obtained when silica nanoparticles were added to Ag/Triton X-100 gels (without HF treatment). Major weight loss about 52 % was observed and left 14 % of silver with silica (Fig. 2d).

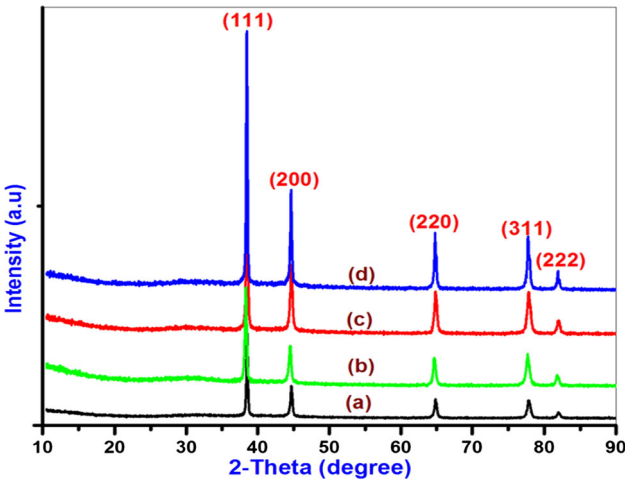

Fig. 3 X-ray diffraction patterns of silver monoliths with Triton X-100 as templates, *a* Ag/Triton X-100 monolith, *b* Ag/Triton X-100/dextran framework, *c* Ag/Triton X-100/TMB monolith and *d* Ag/Triton X-100/Ludox monolith (after HF treatment)

3.2 Powder X-ray diffraction

The composition and phase purity of the as-prepared samples were examined by XRD (Fig. 3). X-ray studies of silver monoliths showed reflections at *d* spacings of 2.37, 2.06, 1.45, 1.23 and 1.18 Å, which correspond to {111}, {200}, {220}, {311} and {222} lattice planes of a face-centered cubic unit cell structures (JCPDS No. 4.783) associated with Fm3 m symmetry. The high crystallinity of the synthesized samples is quite clear from the intense and sharp peaks [46]. From P-XRD, *d* spacing, lattice parameters for all the four synthesized samples were calculated as given in Table 1.

3.2.1 SEM and nitrogen sorption study

SEM images in Fig. 4 depict the morphological behavior of the samples. Figure 4a shows the disordered network of pores with average diameter of 1.5 μm of Ag/Triton X-100. On adding dextran to above gel, pore size increased to 3 μm Fig. 4b, but pore density showed a marked increase in Ag/Triton X-100/dextran than Ag/Triton X-100. As swelling agent TMB was added to Ag/Triton X-100, pore size increased to 3.5 μm Fig. 4c. However, when Ludox was used, the pore size decreased to 1 μm Fig. 4d in Ag/Triton X-100/Ludox framework (after HF treatment). The absence of silica nanoparticles was confirmed by energy-

Table 1 Physicochemical properties and reaction conversion time for the reduction of p-nitrophenol of Ag monoliths synthesized by using Triton X-100 non-ionic surfactant as a sacrificial agent

Sample	"*d*" spacing (Å)	BET surface area (m^2/g)	Average pore diameter (μm)	Pore volume (cm^3/g)	Conversion time (s)
Ag/Triton X-100	2.355	20.451	1.2	0.000387	1550
Ag/Triton X-100/dextran	2.353	32.602	3.0	0.000574	1320
Ag/Triton/X-100/TMB	2.356	44.452	3.5	0.000697	900
Ag/Triton X-100/Ludox (HF treated)	2.357	60.621	1.0	0.062100	750

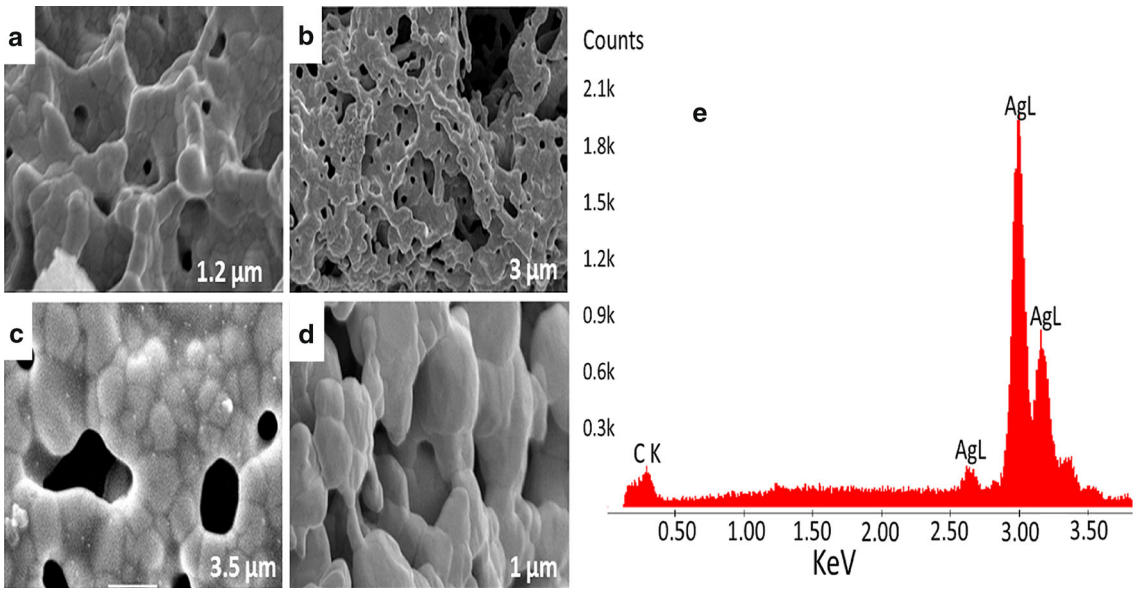

Fig. 4 SEM images of **a** Ag/Triton X-100 sponge, *scale bar* 10 µm, **b** Ag/Triton X-100/dextran, *scale bar* 20 µm, **c** Ag/Triton X-100/TMB, *scale bar* 5 µm. **d** Ag/Triton X-100/Ludox (HF treatment), *scale bar* 2 µm. **e** EDX of Ag/Triton X-100/Ludox (HF treatment) showing absence of silica nanoparticles

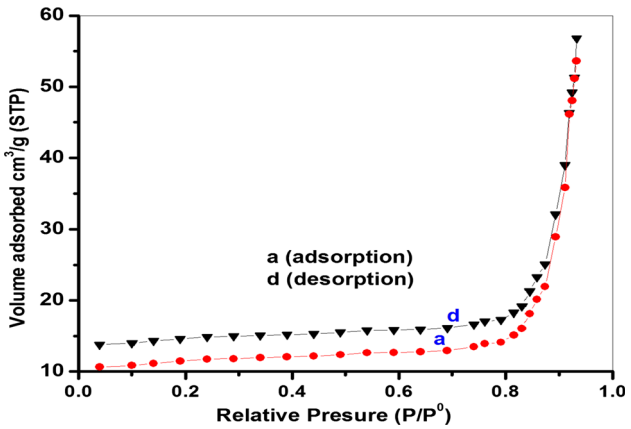

Fig. 5 Nitrogen adsorption–desorption isotherm for silver monolith prepared by the calcination of Ag/Triton X-100/silica nanoparticles (after HF treatment) gel

dispersive X-ray (EDX) analysis Fig. 4e. For further studies, nitrogen sorption isotherms of the synthesized calcined monoliths were closely investigated and displayed sorption isotherm of type II as shown in (Fig. 5) which is the isotherm of Ag/Triton X-100/Ludox (after HF treatment). The sample exhibits type II isotherm of the IUPAC classification which features the macroporous characteristic of the silver monolith [47] with BET surface area of 60 m^2/g highest among the synthesized samples which show a dramatic increase from 20 to 60 m^2/g as given in Table 1. The sorption isotherms show rise when P/P_0 is above 0.8 or close to 1 [48], revealing the existence of macropores which is in complete agreement with SEM results.

3.3 Catalytic performance

A number of catalytic methods have been used to carry out the reduction of nitroaromatics as aminoaromatics like 4-AP are significant intermediates for different industrial products is well documented [45]. Therefore, we used the reduction of 4-NP to 4-AP with an excess amount of $NaBH_4$ as a model system to evaluate the catalytic activity of different silver monoliths at room temperature. As shown in Fig. 6a, 4-NP solution exhibits a strong absorption peak at 317 nm in neutral or acidic conditions at 273 K. When treated with an aqueous solution of $NaBH_4$, it is remarkably red shifted to 400 nm corresponding to the formation of an intermediate nitrophenolate ion. This peak remains unaltered with time, which suggests that the reduction did not take place in the absence of a catalyst Fig. 6b [49].

However, the addition of a small amount (0.06 mg) of the as-prepared different silver monoliths to the above mixture causes fading and ultimate bleaching of the yellow color of the reaction mixture in quick succession. The kinetics could be easily monitored by taking time-dependent UV–vis spectra of this reaction mixture associated with gradual disappearance of peak at 400 nm and a concomitant appearance of a new peak at 302 nm, demonstrating the formation of 4-AP Fig. 7a–d. It clearly shows the excellent catalytic activity of the as-prepared

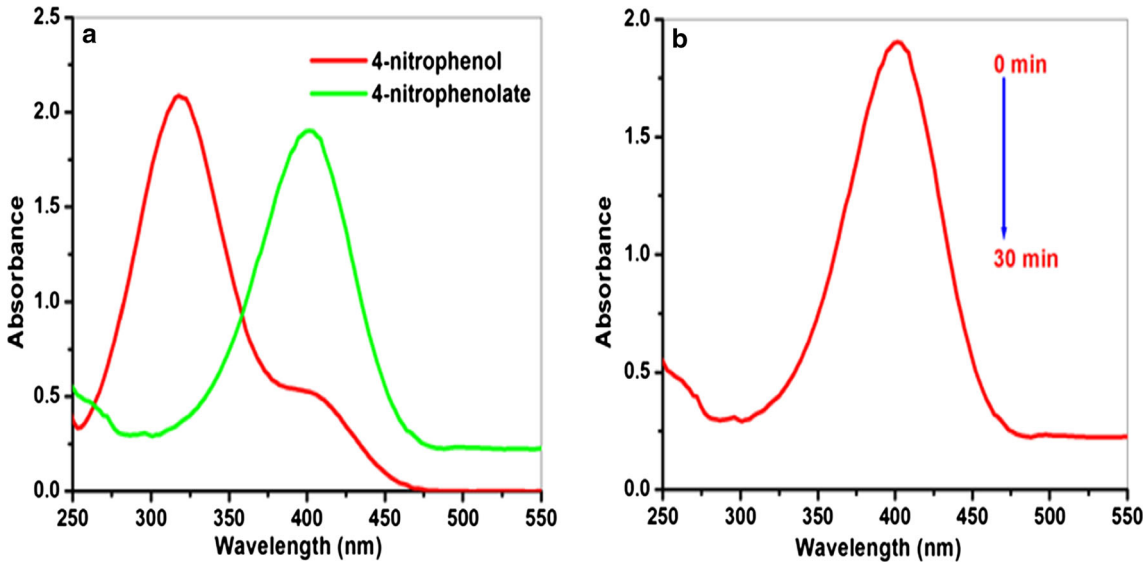

Fig. 6 UV–vis spectra of **a** 4-nitrophenol (4-NP) and 4-nitrophenolate. **b** UV–visible spectra of phenolate ion in absence of catalyst

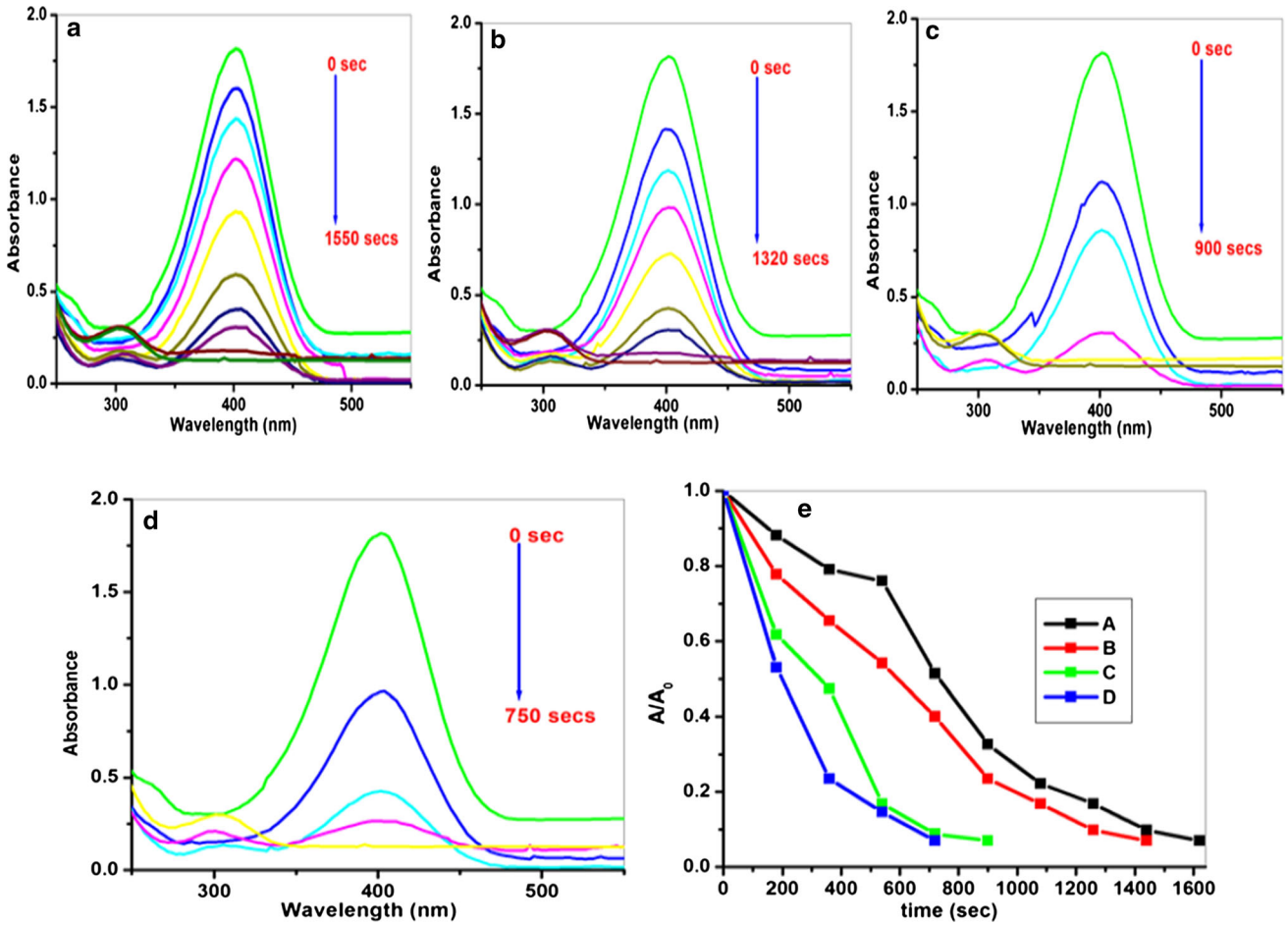

Fig. 7 **a–e** Time-dependent successive UV–Vis spectra showing the reduction of 4-nitrophenol catalyzed by 0.06 mg of different silver monolith catalysts **a** Ag/Triton X-100, **b** Ag/Triton X-100/dextran, **c** Ag/Triton X-100/TMB, **d** Ag/Triton X-100/Ludox (HF treated). **e** Plots of A/A_0 versus time of different Ag monoliths for catalytic reduction of 4-nitrophenol (*A*) Ag/Triton X-100 (*B, C*) Ag/Triton X-100/dextran Ag/Triton X-100/TM (*D*) Ag/Triton X-100/Ludox (HF treated)

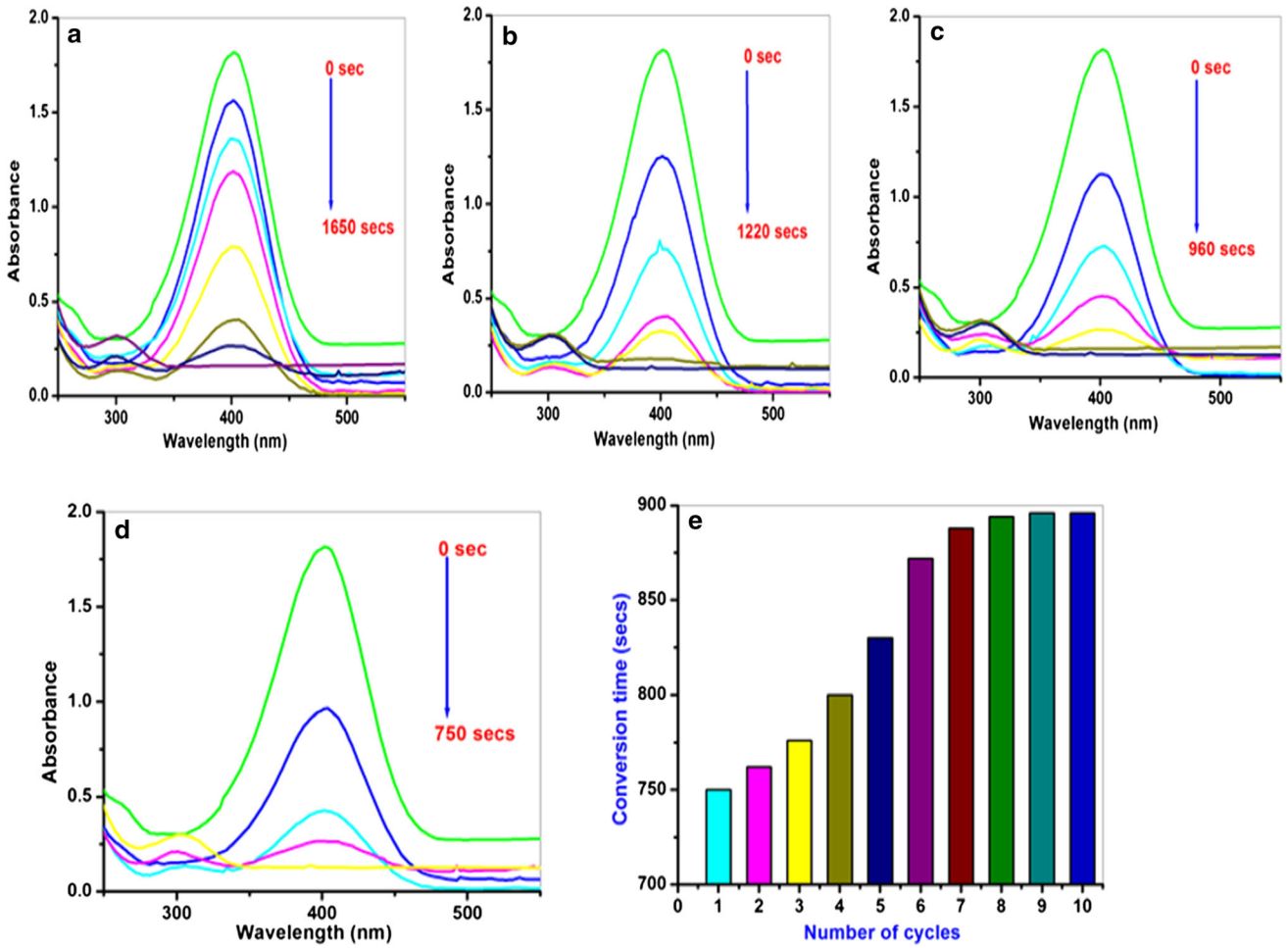

Fig. 8 **a–e** Time-dependent successive UV–vis spectra showing the reduction of 4-nitrophenol catalyzed by different doses of Ag/Triton X-100/Ludox catalyst (**a**) 0.01 mg, (**b**) 0.03 mg, (**c**) 0.04 mg, (**d**) 0.06 mg. **e** Conversion time against number of cycles for 0.06 mg Ag/Triton X-100/Ludox (HF treated)

Table 2 Reaction time for the complete conversion of 4-NP to 4-AP and their rate constants over different doses of Ag/Triton X-100/Ludox (HF treated)

Sample	Weight of catalyst (mg)	Conversion time (s)	Rate constant (s^{-1})
Ag/Triton X-100/Ludox (HF treated)	0.01	1650	4.7×10^{-4}
	0.02	1220	1.0×10^{-3}
	0.04	960	1.4×10^{-3}
	0.06	750	1.7×10^{-3}

HF-treated Ag/Triton X-100/Ludox catalyst as this takes lesser time for the completion of reaction as compared to other synthesized silver monoliths. The larger surface area of this catalyst among the all above tested may be the cause of such an excellent catalytic activity as the heterogeneous catalytic reaction depends on the surface area. Because an excess of $NaBH_4$ was used, pseudo-first-order kinetics with respect to the reduction of 4-NP was set in this case to evaluate the catalytic rate [50–53]. The correlation of reduction is shown by the plot A/A_0 versus time for different catalysts as shown in Fig. 7e. The comparative investigation of the rate of reduction of 4-NP with $NaBH_4$ using different doses of Ag/Triton X-100/Ludox framework (after HF treatment) was also studied. The rate of reaction increases as the concentration of catalyst is increased which is clear from the time-dependent UV–vis spectra shown in Fig. 8a–d. The pseudo-first-order rate constants (Ka) calculated for each used Ag/Triton X-100/Ludox framework (after HF treatment) catalyst dose are given in Table 2. Here, we also made a reusability test for

HF-treated Ag/Triton X-100/Ludox catalyst. From the solution, the used catalyst was separated by centrifugation, washed, dried and used for next operation. After the first cycle, the conversion time, however, slightly increases, but the test clearly confirms that the catalyst is highly active even for tenth cycle as shown in Fig. 8e.

4 Conclusion

We have successfully synthesized a series of silver monoliths by environmentally benign and reliable sol–gel method using Triton X-100 as a sacrificial agent. The additives showed a drastic change in the pore size and surface area of monoliths particularly silica nanoparticles. The calcined silver monoliths displayed a potential catalytic activity against the reduction of 4-nitrophenol which is a serious environmental pollutant to 4-aminophenol which is an important intermediate in the synthesis of various analgesic and antipyretic drugs. Furthermore, the high reusability of the catalysts proved them competitive for the catalysis. Results obtained in this work open an avenue to the fabrication of highly efficient porous silver metal sponges for serving as an ideal platform to study the various heterogeneous catalytic processes. Such interesting porous metal sponges can be expected to have promising potential for applications in electrocatalysis, electrochemical double layer supercapacitors, effective materials for disinfection agents and catalysts in organic synthesis.

Acknowledgments The MUD and GAN highly acknowledge UGC New Delhi for financial assistance as Central University Fellowship (CUF) and MT for RGNF and MB acknowledge DST for providing fellowship. Authors also acknowledge, Head, Department of Chemistry, Sophisticated Instrumentation Center (SIC), Dr. Hari Singh Gour Central University, Sagar, for providing the necessary facilities to carry out this research work.

Compliance with Ethical Standards

Conflict of interest All authors have approved the manuscript and agreed for submitting this original research in this esteemed journal. So, there is no conflict of interest.

References

1. Sayed E, Acc MA (2001) Chem Res 34:257–264
2. Wang L, Luo J, Shan S, Crew E, Yin J, Zhong CJ, Wallek B, Wong SSS (2011) Anal Chem 83:8688–8695
3. Tang S, Vongehr S, Meng X (2010) J Phys Chem C 114:977–982
4. Yamamoto M, Kashiwagi Y, Nakamoto M (2006) Langmuir 22:8581–8586
5. Kim JY, Lee JS (2010) Chem Mater 22:6684–6691
6. Zhang Q, Li W, Moran C, Zeng J, Chen J, Wen LP, Xia Y (2010) J Am Chem Soc 132:11372–11378
7. Netzer NL, Gunawidjaja R, Hiemstra M, Zhang Q, Tsukruk VV, Jiang C (2009) ACS Nano 3:1795–1802
8. Tang B, An J, Zheng X, Xu S, Li D, Zhou J, Zhao B, Xu W (2008) J Phys Chem C 112:18361–18367
9. Halvorson RA, Environ P (2010) J Sci Technol 44:7749–7755
10. Brock SL (2007) Science 317:460
11. Kresge CT, Leonowicz ME, Roth WJ, Vartuli JC, Beck JS (1992) Nature 359:710
12. Hankel M, Jiao Y, Du A, Gray SK, Smith SC (2012) J Phys Chem C 116:6672–6676
13. Schoeld WCE, Bain CD, Badyal JPS (2012) Chem Mater 24:1645–1653
14. Fauth DJ, Gray ML, Pennline HW, Krutka HM, Sjostrom S, Ault AM (2012) Energy Fuels 26:2483–2496
15. Zapilko C, Liang Y, Nerdal W, Anwander R (2007) Chem Eur J 13:3169–3176
16. Shen C, Wang YJ, Xu JH, Wang K, Luo GS (2012) Langmuir 28:7519–7527
17. Xia BY, Ng WT, Wu HB, Wang X, Lou XW (2012) Angew Chem Int Ed 51:7213–7216
18. Lou XW, Archer LA, Yang Z (2008) Adv Mater 20:3987–4019
19. Wang ZY, Luan D, Li CM, Su FB, Madhavi S, Boey F, Lou XW (2010) J Am Chem Soc 132:16271–16277
20. Ding SJ, Chen JS, Wang ZY, Cheah YL, Madhavi S, Hu X, Lou XW (2011) J Mater Chem 21:1677–1680
21. Zhou L, Zhao DY, Lou XW (2012) Angew Chem Int Ed 51:239–241
22. Naikoo GA, Dar RA, Khan F (2014) J Mater Chem A 2:11792–11798
23. Sun FQ, Cai WP, Li Y, Jia LC, Lu F (2005) Adv Mater 17:2872–2877
24. Kim MD, Dergunov SA, Lindner E, Pinkhassik E (2012) Anal Chem 84:2695–2701
25. Yoon S, Lee J, Hyeon T, Oh SM (2000) J Electrochem Soc 147:2507–2512
26. Liu KC, Anderson MA (1996) J Electrochem Soc 143:124–130
27. Lang XY, Yuan HT, Iwasa Y, Chen MW (2011) Scr Mater 64:923–926
28. Liu H, Zhu G (2007) J Power Sour 171:1054–1061
29. Naikoo GA, Dar RA, Thomas M, Sheikh MUD, Khan F (2015) J Mater Sci Mater Electron 26:2403–2410
30. Hubbell JA, Langer R (1995) Chem Eng News 73:42–54
31. Tseng HH, Kumar IA, Weng TH, Lu CY, Wey MY (2009) Desalination 240:40–45
32. Huo Q, Margolese DI, Stucky GD (1996) Chem Mater 8:1147–1160
33. Khan F, Mann S (2009) J Phys Chem C 113:19871–19874
34. Shin KS, Choi JY, Park CS, Jang HJ, Kim K (2009) Catal Lett 133:1–7
35. Comisso N, Cattarin S, Fiameni S, Gerbasi R, Mattarozzi L, Musiani M, Gómez V, Verlato E (2012) Electrochem Commun 25:91–93
36. Narayanan KB, Sakthivel N (2011) J Hazard Mater 189:519–525
37. Lai TL, Yong KF, Yu JW, Chen JH, Shu YY, Wang CB (2011) J Hazard Mater 185:366–372
38. Makovec D, Sajko M, Selišnik A, Drofenik M (2011) Mater Chem Phys 129:83–89
39. Zhang W, Tan F, Wang W, Qiu X, Qiao X, Chen J (2012) J Hazard Mater 217–218:36–42
40. Lu W, Ning R, Qin X, Zhang Y, Chang G, Liu S, Luo Y, Sun X (2011) J Hazard Mater 129:320–326
41. Kkroschwitz JI (1995) Kirk-Othmer encyclopedia of chemical technology, vol 2, 4th edn. Wiley, New York, p 580
42. Liu P, Zhao M (2009) Appl Surf Sci 255:3989–3993
43. Kojima Y, Suzuki K, Fukumoto K, Sasaki M, Yamamoto T, Kawai Y, Hayashi H (2002) Int J Hydrog Energy 27:1029–1034

44. Liu CH, Chen BH, Hsueh CL, Ku JR, Jeng, Tsau F (2009) Int J Hydrog Energy 34:2153–2163
45. Gao S, Jia X, Yangb J, Wei X (2012) J Mater Chem 22:21733–21739
46. Cao Y, Fan J, Bai L, Hu P, Yang G, Yuan F, Chen Y (2010) Cryst Eng Comm 12:3894–3899
47. Yan J, Wei T, Fan Z, Qian W, Zhang M, Shen X, Wei F (2010) J Power Sour 195:3041–3046
48. Wu ZS, Parvez K, Feng X, Mullen K (2013) Nat Commun 4:2487
49. Hayakawa K, Yoshimura T, Esumi K (2003) Langmuir 19:5517–5521
50. Mei Y, Sharma G, Lu Y, Ballauff M, Drechsler M, Irrgang T, Kempe R (2005) Langmuir 21:12229–12234
51. Mei Y, Lu Y, Polzer F, Ballauff M (2007) Chem Mater 19:1062–1069
52. Panigrahi S, Basu S, Praharaj S, Pande S, Jana S, Pal A, Gosh SK, Pal T (2007) J Phys Chem C 111:4596–4605
53. Gao S, Jia X, Li Z, Chen Y (2012) J Nanopart Res 14:748